# Efficiency Maximization in Wireless Power Transfer Systems for Resonance Frequency Mismatch

Helanka Weerasekara, Katsuhiro Hata, Takehiro Imura, Hiroshi Fujimoto, Yoichi Hori
*Graduate school of Engineering*
*The University of Tokyo*
Kashiwa, Japan
weerasekara.helanka18@ae.k.u-tokyo.ac.jp

***Abstract*—In wireless power transfer (WPT), resonance frequency mismatch occurs, when primary and secondary sides have different resonance frequencies due to inductance and capacitance change. This paper examines on the transmission efficiency of the WPT systems, those are influenced by the resonance frequency mismatch. It is proved that the transmission efficiency is influenced by the operating source frequency and secondary resonance frequency, and not lean on the primary resonance frequency, by conducting both the logical analysis and the experiment. Furthermore, transmission efficiency maximization of WPT system with resonance frequency mismatch is proposed by optimizing the load resistance in this paper. In addition, the validity of the proposed method was confirmed by numerical simulation and experiment.**

***Index Terms*—Wireless power transfer, resonance frequency mismatch, transmission efficiency, optimum load resistance**

## I. Introduction

In recent years, electric vehicle (EV) is considered as the aspiration for zero emissions. However, as EV can perform only short-distance cruising with one charge and have some problems of long charging time, many studies are performed on the in-motion wireless power transfer (WPT) of EV [1]–[3].

The technology of coupled magnetic resonant helix coils is proposed, to deliver power over 2 meters with efficiency near 50% and light a bulb of 60 Watt successfully in 2007 [4]. In WPT system, the power is transferred from the transmitting coil to the receiving coil by inducing the voltage in receiving coil from magnetic field generation in transmitting coil. Previous studies have been conducted assuming that the primary resonance frequency, the secondary resonance frequency, and the operation frequency are same, to gain the maximum transmission efficiency [5]–[8].

However, in practice, the resonance frequency mismatch occurs when the inductance of the coil and capacitance of the capacitor changes, due to manufacturing errors, climate change and temperature variation. Using superior coils and capacitors with less errors is one of the solutions to avoid the resonance frequency mismatch condition. Still, these solutions also have problems, such as high cost, sorting man-hours and some principle matters, thus it is necessary to analyze the WPT circuit with resonance frequency mismatch, to solve the parameter variation problem. Moreover, the variation of the load resistance will also affect the transmission efficiency of the WPT system [9]. The transmission characteristics of various WPT systems can be mainly compared by the source frequency and resonance frequency [10].

A novel analysis method of transmission efficiency for resonance frequency mismatch in WPT system is proposed, considering on source frequency, resonance frequency and load resistance variation, in this paper. The proposed method is first discovered the influence of source frequency, and primary and secondary resonance frequency to transmission efficiency by theoretical analysis, and confirmed by experiment, for a constant load WPT circuit topology. Then, the transmission efficiency maximization method for WPT systems with resonance frequency mismatch is described by optimizing the load resistance. Finally, the proposed method is confirmed at different resonance frequencies by logical analysis results and experiment.

## II. WPT circuit analysis on transmission efficiency

In this paper, an SS-type WPT circuit is considered to analyze the WPT system with resonance frequency mismatch as shown in Fig. 1. Primary resonance frequency $f_1$ is related with primary side inductance $L_1$ and capacitance $C_1$, and secondary resonance frequency $f_2$ is related with secondary side capacitance inductance $L_2$ and $C_2$, are defined as follows:

$$f_1 = \frac{1}{2\pi\sqrt{L_1 C_1}}, \quad f_2 = \frac{1}{2\pi\sqrt{L_2 C_2}}. \tag{1}$$

To achieve high efficiency transmission shown in Fig. 1, typically, many studies are conducted, assuming that the operating source frequency $f_0$ is equal with both resonance frequencies of the primary and secondary sides ($f_0 = f_1 = f_2$) [4]–[7].

However, when resonance frequency mismatch is taken into account, the above-mentioned condition is not true, and all the equations, simulation and experiment results in this paper

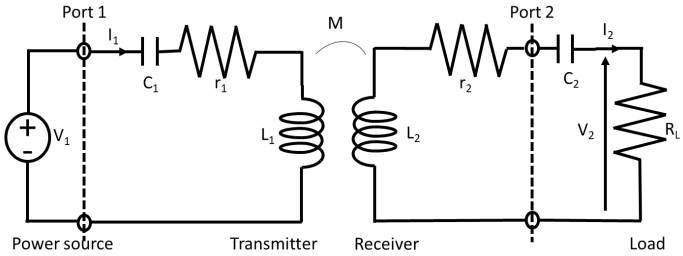

Fig. 1: Circuit diagram of SS type WPT circuit.

TABLE I: Parameters of transmitting and receiving coil

| Parameter | Transmitter | Receiver |
|---|---|---|
| Resisitance $R_1$, $R_2$ | 1.00 Ω | 1.05 Ω |
| Inductance $L_1$, $L_2$ | 617 $\mu$H | 617 $\mu$H |
| Coupling coefficient $k$ | 0.06 | |
| Transmitting gap | 300 mm | |
| Outer diameter | 440 mm | |
| Number of turns | 50 turns | |

TABLE II: Capacitences used for experimental verifications

| $f_1$, $f_2$[kHz] | 80.9 | 82.6 | 84.9 | 86.5 | 89.0 |
|---|---|---|---|---|---|
| $C_1$, $C_2$[nF] | 6.26 | 6.02 | 5.69 | 5.49 | 5.18 |

are achieved, according to the resonance frequency mismatch condition ($f_0 \neq f_1 \neq f_2$).

In Fig. 1, output voltage $V_2$, input current $I_1$, output current $I_2$ are defined as shown in (3), (4) and (5) respectively, where $V_1$, $R_1$, $R_2$, $R_L$, $\omega_0$, $\omega_1$, $\omega_2$, $M$ are input voltage, transmitter coil resistance, receiver coil resistance, load resistance, operating angular frequency, primary resonance angular frequency, secondary resonance angular frequency and mutual inductance of the primary and secondary coil,respectively. Then, transmission efficiency $\eta$ is calculated by (6), expressed as (7).

$$V_2 = R_L I_2. \tag{2}$$

$$I_1 = \frac{\left(R_2+R_L+j\omega_2 L_2\left(\frac{\omega_0}{\omega_2}-\frac{\omega_2}{\omega_0}\right)\right)V_1}{\left\{R_1+j\omega_1 L_1\left(\frac{\omega_0}{\omega_1}-\frac{\omega_1}{\omega_0}\right)\right\}\left\{R_2+R_L+j\omega_2 L_2\left(\frac{\omega_0}{\omega_2}-\frac{\omega_2}{\omega_0}\right)\right\}+{\omega_0}^2M^2} \tag{3}$$

$$I_2 = \frac{j\omega_0 M V_1}{\left\{R_1+j\omega_1 L_1\left(\frac{\omega_0}{\omega_1}-\frac{\omega_1}{\omega_0}\right)\right\}\left\{R_2+R_L+j\omega_2 L_2\left(\frac{\omega_0}{\omega_2}-\frac{\omega_2}{\omega_0}\right)\right\}+{\omega_0}^2M^2}. \tag{4}$$

$$P_1 = \mathrm{Re}\left\{V_1\bar{I}_1\right\}, \quad P_2 = \mathrm{Re}\left\{V_2\bar{I}_2\right\}. \tag{5}$$

$$\eta = \frac{P_2}{P_1} = \frac{{\omega_0}^2M^2R_L}{R_1(R_2+R_L)^2+R_1\omega_2^2L_2^2\left(\frac{\omega_0}{\omega_2}-\frac{\omega_2}{\omega_0}\right)^2+{\omega_0}^2M^2(R_2+R_L)} \tag{6}$$

According to (7), the transmission efficiency is influenced by the operating angular frequency and secondary resonance angular frequency, and not lean on the primary resonance angular frequency.

## III. Verification with Constant Load Resistance

### A. Validation Parameters

The numerical analysis and experiment were conducted with the transmitting and receiving coil parameters as indicated in Tab. I. The Transmitting (primary side) and receiving (secondary side) coil in Fig. 2, are used for the experiment. Here, the load resistance is set as 10 Ω.

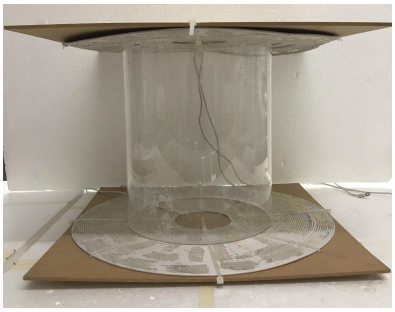
Fig. 2: Transmitting and receiving coil.

The simulation is performed, when the resonance frequency range is varied from 81 kHz to 89 kHz. For the experiment verification, only five different resonance frequencies (81 kHz, 83 kHz, 85 kHz, 87 kHz, 89 kHz) are chosen. The resonance frequency variation situation for the experiment, is created by changing the primary and secondary side capacitances as shown in Tab. II, those are calculated according to (1).

### B. Theoretical Verifications

In this chapter, numerical analysis is discussed on the transmission efficiency (7) obtained in section II. Figure 3 shows the theoretical transmission efficiency graphs for various operating source frequencies. The theoretical calculations are done at various operating source frequencies. The yellow color space represents the high transmission efficiency range, moves vertically according to the secondary resonance frequency and it remains same range of yellow color with the horizontal axis of primary resonance frequency.

### C. Experimental Verification

In the experiment, the Vector Network Analyzer (VNA, E5061B ENA Series Keysight) was connected to port 1 and port 2 shown in Fig.1, and the efficiency from the primary side to the secondary side was measured. The coils used for the measurements are shown in Fig. 2. The primary side capacitance $C_1$ is changed by replacing the capacitors. On the other hand, the secondary side capacitance $C_2$ is varied by VNA. Load resistance of 10 Ω also set in VNA.

The experiment results graphs are shown in Fig. 4. From Fig. 4, the high transmission efficiency range is varied according to the secondary resonance frequency. Theoretical and experimental results have the same behavior of the transmission efficiency variation to resonance frequency mismatch. Therefore, it is proved, that the logical analysis method performed in the section II and section III(B) is applicable.

## IV. Load Optimization for Efficiency Maximization

### A. Maximum Efficiency Condition

In this section, transmission efficiency maximization method is proposed according to the variation of load resistance, when the WPT system is with resonance frequency mismatch condition. By taking derivatives of (7) with respect to $R_L$, the optimum load resistance $R_{L\mathrm{opt}}$ that maximize the efficiency $\eta$, can be found as follows:

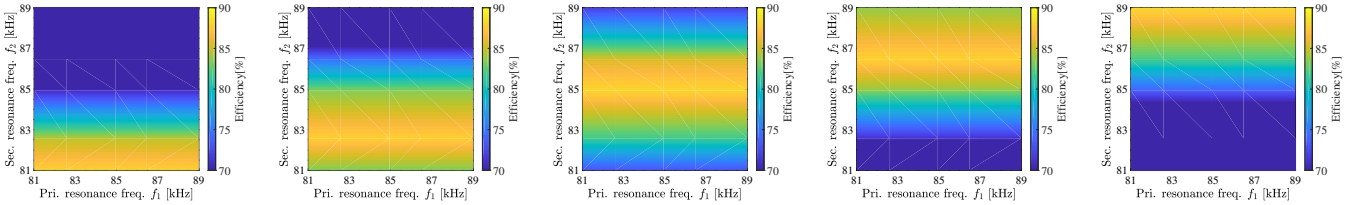


(a) $f_0$ = 81 kHz (b) $f_0$=83 kHz (c) $f_0$=85 kHz (d) $f_0$=87 kHz (e) $f_0$=89 kHz

Fig. 3: Theoretical results of transmission efficiency. (a) $f_0$=81 kHz, (b) $f_0$=83 kHz, (c) $f_0$=85 kHz, (d) $f_0$=87 kHz, (e) $f_0$=89 kHz

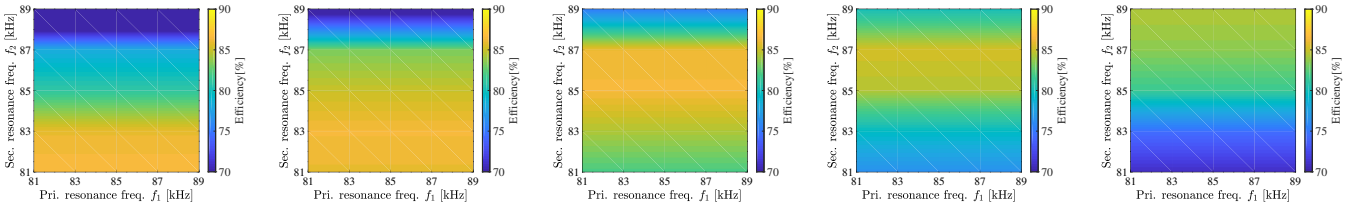


(a) $f_0$ = 81 kHz (b) $f_0$=83 kHz (c) $f_0$=85 kHz (d) $f_0$=87 kHz (e) $f_0$=89 kHz

Fig. 4: Experimental results of transmission efficiency. (a) $f_0$=81 kHz, (b) $f_0$=83 kHz, (c) $f_0$=85 kHz, (d) $f_0$=87 kHz, (e) $f_0$=89 kHz

$$\left.\frac{\partial \eta}{\partial R_L}\right|_{R_L=R_{L\mathrm{opt}}} = 0$$

$$\Leftrightarrow R_{L\mathrm{opt}} = \sqrt{R_2^2 + \omega_2^2 L_2^2 \left(\frac{\omega_0}{\omega_2} - \frac{\omega_2}{\omega_0}\right)^2 + \omega_0^2 M^2 \frac{R_2}{R_1}}. \quad (7)$$

From (8), the optimum load resistance $R_{L\mathrm{opt}}$ changes according to the operating source angular frequency $\omega_0$ and the secondary resonance angular frequency $\omega_2$, and have no influence from the primary resonance angular frequency $\omega_1$.

Figure 5 shows the variation of optimum load resistance $R_{L\mathrm{opt}}$, when operating source frequency and secondary resonance frequency are changed. $R_{L\mathrm{opt}}$ has the minimum value, when the secondary resonance frequency is equal to the operating source frequency.

In addition, large fluctuations of $R_{L\mathrm{opt}}$ are driven, when the resonance frequency mismatch occurs, become obvious as shown in Fig. 5.

### B. Theoretical Verification

As shown in Fig. 6, the theoretical calculations are performed at different values of primary and secondary resonance frequencies to obtain the influence of resonance frequency mismatch to the maximum transmission efficiency. The maximum transmission efficiency graphs for various operating source frequencies are drawn for resonance frequency mismatch, as shown in Fig. 6. The maximum efficiency is influenced by the vertical axis of secondary resonance frequency and maximum efficiency remains same with the horizontal axis of primary resonance frequency.

### C. Experimental Verification

Here, only the load resistance condition is different from the previous experiment verification mentioned in section III. The optimum load resistance $R_{L\mathrm{opt}}$ values, which are calculated according to (7) are adjusted by VNA. Fig. 7 shows the maximum transmission efficiency graphs of the experiment.

According to Fig. 7, the yellow color range which represents the maximum efficiency values, moves vertically according to the secondary resonance frequency and however, the primary resonance frequency mismatch is not related with the yellow range. Therefore, the theoretical results and the experimental results agree well. Moreover, the yellow color range, which represents the high transmission efficiency area, is increased at all the five operating source frequencies mentioned above in Fig. 7 compared to Fig. 4.

### D. Discussion

Measurement results and theoretical results are almost same in appearance in both conditions, when the load resistance $R_L$ is fixed, and optimum load resistance $R_{L\mathrm{opt}}$ is considered for the WPT system with resonance frequency mismatch. According to both theoretical and measurement graphs, high transmission efficiency is obtained when operating source frequency and secondary resonance frequency is nearly equal. Maximum transmission efficiency is gained by optimizing load resistance $R_{L\mathrm{opt}}$. However, transmission efficiency of measurement results are only different in high transmission efficiency color range, compared with the theoretical results in section III and section IV. This difference may be caused by because of neglecting the equivalent series resistances (ESRs) values of capacitors and the components.

## V. Conclusion

This paper presented on the transmission efficiency variation on the WPT system with resonance frequency mismatch. The WPT circuit analysis is performed to examine the influence of source frequency, primary and secondary resonance frequency to transmission efficiency. Additionally, This paper proposed

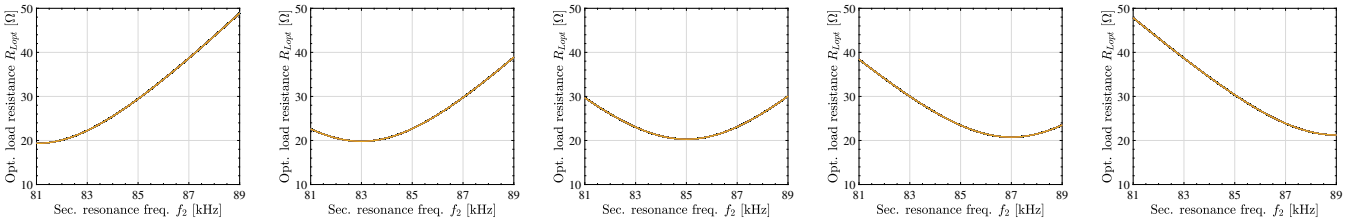


(a) $f_0$ = 81 kHz (b) $f_0$=83 kHz (c) $f_0$=85 kHz (d) $f_0$=87 kHz (e) $f_0$=89 kHz

Fig. 5: optimum load resistance $R_{L\mathrm{opt}}$ variation.

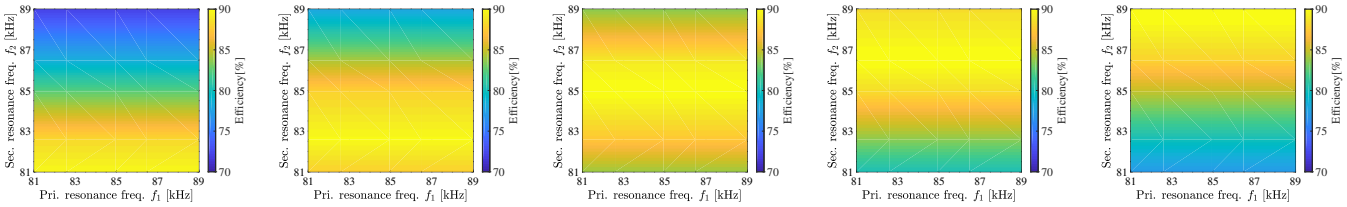


(a) $f_0$ = 81 kHz (b) $f_0$=83 kHz (c) $f_0$=85 kHz (d) $f_0$=87 kHz (e) $f_0$=89 kHz

Fig. 6: Theoretical results of transmission efficiency on resonance frequency mismatch ($R_L$ = $R_{L\mathrm{opt}}$).

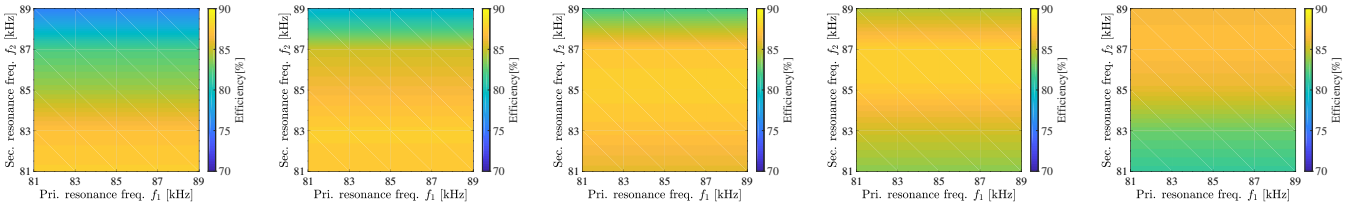


(a) $f_0$ = 81 kHz (b) $f_0$=83 kHz (c) $f_0$=85 kHz (d) $f_0$=87 kHz (e) $f_0$=89 kHz

Fig. 7: Experimental results of transmission efficiency on resonance frequency mismatch ($R_L$ = $R_{L\mathrm{opt}}$).

efficiency maximization based on load optimization considering on resonance frequency mismatch.

It is confirmed that the transmission efficiency is influenced only by the secondary resonance frequency and does not depend on the primary resonance frequency. Maximum transmission efficiency is gained by optimizing load resistance $R_{L\mathrm{opt}}$ according to the operating source frequency and the secondary resonance frequency. Therefore, when the resonance frequency mismatch occurs, the secondary resonance frequency is the key target to achieve the maximum efficiency.

Study on implementation issues of frequency control and examination on transmission power and power factor characteristics will be studied in the future.

## ACKNOWLEDGMENT

This work was partly supported by JSPS KAKENHI Grant Number 16J06942 and 17H04915.

## REFERENCES

[1] Siqi Li, and Chunting Chris Mi, "Wireless Power Transfer for Electric Vehicle Applications," IEEE Journal of Emerging and Selected Topics in Power Electronics, Vol. 3, pp.4–17, March 2018.

[2] Chunting Chris Mi, Giuseppe Buja, Su Y. Choi, Chun T. Rim, "Modern Advances in Wireless Power Transfer Systems for Roadway Powered Electric Vehicles," IEEE Transactions on Industrial Electronics, Vol. 63, pp. 6533—6545, June 2016.

[3] Devendra Patil, Matthew K. McDonough, John M. Miller, Babak Fahimi, Poras T. Balsara, "Wireless Power Transfer for Vehicular Applications:Overview and Challenges," IEEE Transactions on Transportation Electrification, Vol. 4, pp. 3—37, December 2018.

[4] A. Kurs, A. Karakis, R. Moffatt, J. D. Joannopoulos, P. Fisher, and M.Soljacic, "Wireless power transmission via strongly coupled magnetic resonances," Science, Vol. 317, pp. 83–86, July 2007.

[5] Zhongzheng Lin, Junhua Wang, Zhijian Fang, Meilin Hu, Changsong Cai, Junkun Zhang, "Coil Design and Measurements of Automotive Magnetic Resonant Wireless Charging System for High-Efficiency and Low Magnetic Field Leakage," IEEE Transactions on Microwave Theory and Techniques, Vol. 64, pp. 383–400, February 2016.

[6] Yao-Ching Hsieh, Zhong-Rong Lin, Ming-Cheng Chen, Hsin-Che Hsieh, Yu-Chen Liu, and Huang-Jen Chiu, "High-Efficiency Wireless Power Transfer System for Electric Vehicle Applications," IEEE Transactions on Circuits and Systems, Vol. 64, pp. 942—946, August 2017.

[7] Yiming Zhang, Ting Lu, Zhengming Zhao, Fanbo He, Kainan Chen, and Liqiang Yuan, "Selective Wireless Power Transfer to Multiple Loads Using Receivers of Different Resonant Frequencies," IEEE Transactions on Power Electronics, Vol. 30, pp. 6001—6005, August 2014.

[8] Yeong H. Sohn, Bo H. Choi, Eun S. Lee, Gyu C. Lim, Gyu-Hyeong Cho, Chun T. Rim, "General Unified Analyses of Analyses of Two-Capacitor Inductive Power Transfer Systems: Equivalence of Current-Source SS and SP Compensations," IEEE Transactions on Power Electronics, Vol. 30, pp. 6030–6045, November 2015.

[9] Dukju Ahn, Seongmin Kim, Jungick Moon, and In-Kui Cho, "Wireless Power Transfer With Automatic Feedback Control of Load Resistance Transformation," IEEE Transactions on Power Electronics, Vol. 31, pp. 7876–7886, December 2015.

[10] Takehiro Imura, and Yoichi Hori, "Maximizing Air Gap and Efficiency of Magnetic Resonant Coupling for Wireless Power Transfer Using Equivalent Circuit and Neumann Formula," IEEE Transactions on Power Electronics, Vol. 58, pp. 4746–4752, February 2011.